states are also forbidden. Whether or not ZnS represents an unusual case could be decided experimentally by a more careful analysis of the $n_1=3$ states in both CdSe and CdS.

At present there are no reliable experimental mass values for ZnS with which we can compare our results. Estimates of the effective electron mass using standard $\mathbf{k}\cdot\mathbf{p}$ perturbation theory have been made however, by ourselves and Cardona.[16] In the latter calculation the effect of a higher conduction band on the electron effective mass was considered, and a value of $m_e=0.39$ was found. Now this is to be compared with $m_e=0.28$ as found in this series of experiments. The discrepancy of about 25% may be due to a combination of factors. First there is the inherent error of at least 10% in our determination of the electron mass. Secondly, we have neglected the effects of the interband mixing on the exciton Hamiltonian and evaluated the band parameters in terms of a simple single-conduction-band–single-valence-band model. Finally, there exists the possibility that the interband matrix elements involved in the $\mathbf{k}\cdot\mathbf{p}$ estimates of the electron effective mass may not be equal for all the Group II–VI compounds. Considering these factors, we believe that no definite conclusions can be drawn from the discrepancy between our measured electron mass and the calculated value.

PHYSICAL REVIEW VOLUME 153, NUMBER 3 15 JANUARY 1967

Lattice Dynamics of Sodium Fluoride

W. J. L. BUYERS*
Chalk River Nuclear Laboratories, Atomic Energy of Canada Limited, Chalk River, Ontario, Canada
(Received 8 August 1966)

Phonons in sodium fluoride have been studied at room temperature using inelastic neutron scattering techniques. Consistent results were obtained using a cold neutron time-of-flight apparatus and a triple-axis spectrometer. The time-of-flight results were interpolated on to symmetry directions from the observed scattering surfaces. The frequencies in units of 10^{12} sec^{-1} of some typical phonons are: TA(0,0,1), $\nu=4.39\pm0.04$; LO(0,0,0.984), $\nu=8.52\pm0.15$; LA(0,0,0.972), $\nu=7.94\pm0.18$; TO(0.488, 0.488, 0.488), $\nu=6.19\pm0.07$. The optical branches extrapolated to small wave vector are in agreement with the infrared absorption frequency and the Lyddane-Sachs-Teller relation. Hardy and Karo's deformation-dipole model is in agreement with the results to within 6%, but the rigid-ion model differs by as much as 19%. The results are well fitted by a shell model containing nine parameters in which the ionic charge is 0.91.

1. INTRODUCTION

ALKALI halides have been the subject of many theoretical and experimental investigations of the dispersion relation for vibrational modes. Models of the solid have been developed which facilitate the calculation of dispersion relations without recourse to consideration of the fundamental theory underlying the atomic interactions. The extremely simple Born-Mayer model used by Kellerman[1] was very successful in describing the specific heat, while the various versions of the theory in the dipole approximation, reviewed by Cochran,[2] are able to resolve difficulties in the optical and dielectric behavior of the solid that existed in the earlier work. The most complete confirmation of the reliability of a particular model has been carried out on NaI and KBr by neutron spectroscopy,[3] while NaCl has been the subject of a recent x-ray investigation.[4] It was found in these studies that a general description of the observed dispersion relations was obtained when models such as the simple shell model[5] or the deformation-dipole model,[6] whose parameters were fitted to long-wavelength data, were compared with the scattering results. If, on the other hand, a model was fitted to the observed frequencies, much better agreement could be obtained, often within the experimental accuracy, but only at the expense of losing the simple picture given by the model.[3]

In NaI, NaCl, and KBr, the polarizability of the crystal is higher than the average for alkali halides, and the crystal polarizability[7] of the negative ion is considerably greater than that of the positive ion. It is therefore of interest to see if, in a crystal of low polarizability, whose ions are comparable in size, the simple version of the theory for alkali halides is more satisfactory. Sodium fluoride is well suited for this study. It was also chosen because it has favorable properties for x-ray as well as neutron scattering, and could thus

* Part of this work was performed at the Department of of Natural Philosophy, University of Aberdeen, Scotland.

[1] E. W. Kellerman, Phil. Trans. Roy. Soc. **A238**, 513 (1940).

[2] W. Cochran, in *Lattice Dynamics*, edited by R. F. Wallis (Pergamon Press, Inc., New York, 1965).

[3] R. A. Cowley, W. Cochran, B. N. Brockhouse, and A. D. B. Woods, Phys. Rev. **131**, 1030 (1963); A. D. B. Woods, W. Cochran, and B. N. Brockhouse, *ibid.* **119**, 980 (1960).

[4] W. J. L. Buyers and T. Smith, Phys. Rev. **150**, 758 (1966).

[5] W. Cochran, Phil. Mag. **5**, 1082 (1959).

[6] A. M. Karo and J. R. Hardy, Phys. Rev. **129**, 2024 (1963).

[7] J. Tessman, A. Kahn, and W. Shockley, Phys. Rev. **92**, 890 (1953).

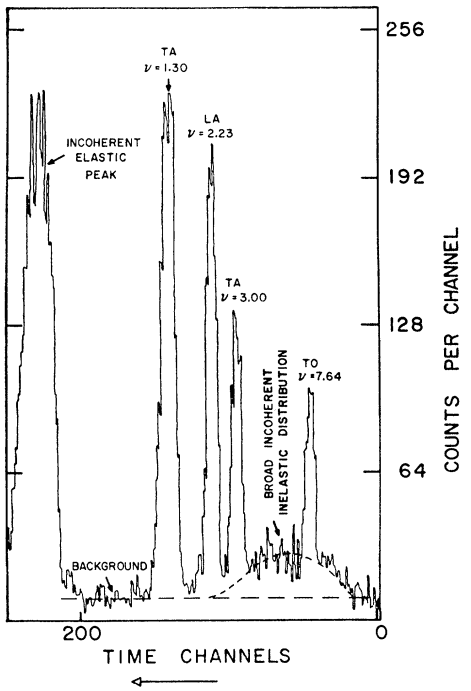

FIG. 1. Time-of-flight spectrum for sodium fluoride. Zero on the time-channel axis corresponds to a flight time between sample and detector of 63 channels. The broken lines indicate how the background and the incoherent inelastic distribution were fitted. The frequencies of the inelastic peaks are given in units 10^{12} cps.

be the subject of an investigation[8] currently being carried out using the x-ray technique.

In Sec. 2 of this paper the experiment is described. In Sec. 3 the results are presented, compared with the theories of Karo and Hardy (Sec. 3.1), and fitted to several versions of the shell model (Sec. 3.2).

2. EXPERIMENTAL

Phonons in a single crystal of NaF at room temperature have been studied by using both a time-of-flight apparatus and a triple-axis spectrometer to measure the energy distribution of inelastically scattered neutrons. The measurements were made on the "Dido" reactor at the Atomic Energy Research Establishment Harwell. The phonon frequency ν and wave vector $\mathbf{q}$ are inferred from conservation of energy and crystal momentum when neutrons of energy E_0 and wave vector $\mathbf{k}_0$ are scattered by a single excitation to the state $(E_1,\mathbf{k}_1)$. If $\hbar\mathbf{Q}$ is the momentum transfer to the crystal, the process is described by

$$E_0-E_1=(\hbar^2/2m_N)(k_0^2-k_1^2]=\pm h\nu \quad (1)$$

$$\hbar\mathbf{Q}=\hbar(\mathbf{k}_0-\mathbf{k}_1)=\hbar(\mathbf{G}+\mathbf{q}), \quad (2)$$

where $\mathbf{G}$ is reciprocal lattice vector, m_N is the mass of the neutron, and the upper sign in Eq. (1) applies for neutron energy loss.

[8] J. D. Pirie and T. Smith (to be published).

The sodium fluoride sample was a high purity (few ppm), single crystal whose mosaic spread was less than the resolution of an x-ray beam of 15 min. horizontal divergence. A cylinder 2 in. in diameter with a ⟨110⟩ axis was cut from a 4-in.-diam. boule.

2.1. Time-of-Flight Method

Time-of-flight measurements in which 4 Å neutrons gained energy from the crystal were made using the cold neutron apparatus, described in detail elsewhere.[9,10]

Sharp neutron groups were observed in the time-of-flight spectra as shown in Fig. 1. A typical peak height after 12 h counting time was 100 counts per 8 μsec time channel at an energy transfer of 7×10^{12} sec^{-1}, in the presence of a back-ground of 20 counts per channel. The full width at half-maximum of the peaks in Fig. 1 is approximately 5% of the time of flight from sample to detector.

The $(\bar{1}10)$ scattering plane of the reciprocal lattice is shown in Fig. 2, with the positions of the observed neutron groups from six typical runs indicated. The frequencies of the neutron groups are obtained by fitting Gaussians to the peaks. The effect of noise and incoherent scattering on the frequencies of the coherent neutron groups is practically eliminated by simultaneously fitting a flat background to the noise, and a broad low Gaussian to the incoherent scattering. It may be seen from Fig. 1 that this method gave a very satisfactory description of the observed time-of-flight spectrum. The peak fitting was performed on an electronic computer using programs written by Peckham.[11]

The above procedure yielded 900 fitted Gaussians, of which 200 were finally rejected. A peak was con-

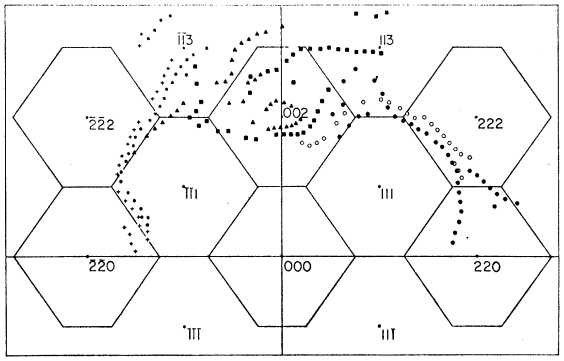

FIG. 2. Typical scattering surfaces in sodium fluoride. Similar points belong to the same crystal orientation but different scattering angles. Each set of points belongs to a different crystal orientation. Any one point gives the position in reciprocal space where a scattered neutron group with energy and momentum satisfying Eqs. (1) and (2) has been observed.

[9] G. Peckham, in *Lattice Dynamics*, edited by R. F. Wallis (Pergamon Press Inc., New York, 1965), p. 49.

[10] D. Harris, S. J. Cocking, P. A. Egelstaff, and F. J. Webb, in *Inelastic Scattering of Neutrons in Solids and Liquids* (International Atomic Energy Agency, Vienna, 1963), p. 107.

[11] G. Peckham, thesis, Cambridge University, 1964 (unpublished).

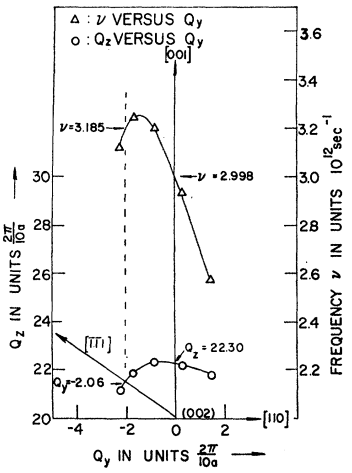

FIG. 3. Method of interpolation of scattering surfaces on to symmetry directions. The numbers at the left of the figure refer to the curve of Q_z versus Q_y, while those at the right refer to ν versus Q_y. From the lower curve (the scattering surface) the coordinates in reciprocal space (Q_z,Q_y) of phonons with wave vectors in the $[\bar{1}\bar{1}1]$ and [001] directions are found to be (21.5, −2.06) and (22.30, 0.0), respectively. The corresponding values of the frequency ν in units 10^{12} sec^{-1}, are then found, by interpolation on the curve of ν versus Q_y at these values of Q_y, to be 3.815 and 2.998, respectively. The broken line is drawn at $Q_y=-2.06$ to facilitate this interpolation.

sidered unsatisfactory if it arose from more than one branch of the dispersion relations, was severely distorted by the scattering geometry or was excessively broad.

The foregoing analysis provides a set of phonon frequencies for wave vectors in more or less random directions throughout the (110) plane of the reciprocal lattice. Where suitable scattering surfaces[12] are clearly defined, it is possible to use them to interpolate, or in some cases to extrapolate the results, so that dispersion curves in symmetry directions are obtained. In general this procedure was found to be satisfactory, in that symmetry phonons were obtained with frequencies as accurately known as those of the original phonons from which the interpolation was made. Figure 3 illustrates how the position in reciprocal space of a phonon in a symmetry direction may be found from a plot of Q_z versus Q_y. One might then obtain the value of ν from Eqs. (1) and (2). In practice, since ν was available from the fitting program for each point, a more rapid and equally accurate method for finding ν in the symmetry direction was used. This consisted of a second interpolation on a plot of ν versus Q_y at the value of Q_y found for the symmetry direction. This graphical method, using common abscissas Q_y for the plots of ν and Q_z, respectively, is shown in Fig. 3 for a case where interpolation was possible on to both the [001] and $[\bar{1}\bar{1}1]$ directions from a single scattering surface.

[12] C. Kittel, *Quantum Theory of Solids* (John Wiley & Sons, Inc., New York, 1963), p. 377.

2.2. Triple-Axis Spectrometer

Although some 700 phonons were measured using the time-of-flight method, sufficient data were not present for certain regions of the dispersion curves. To complete the measurements, 16 phonons were obtained at constant **Q**,[13] using the Harwell triple-axis spectrometer.[14] The spectrometer was operated at neutron energy loss, and employed the (111) plane of an aluminum crystal to analyze the scattered neutron beam. Phonons were studied at points in reciprocal space where their structure factors, based on the deformation dipole model of Karo and Hardy,[6] were expected to be favorable. Well-focused phonons were obtained for the TA[100] branch using a fixed incident frequency of 6.7×10^{12} sec^{-1} (wavelength 1.72 Å). The remaining measurements were carried out with an incident frequency of 13.7×10^{12} sec^{-1} (wavelength 1.20 Å). The phonons obtained in this way were in agreement with those from the time-of-flight method where comparison could be made. The largest discrepancy was 2.7 standard deviations for the LO branch at [0,0,0.578]. Near the zone boundary in the same branch, the difference was only 0.8 standard deviations. The triple-axis frequencies were usually more reliable than those from the time-of-flight method due to their comparative freedom from systematic errors.

3. DISCUSSION OF RESULTS

The dispersion curves for phonons propagating in the $\Delta[00\zeta]$, $\Lambda[\zeta\zeta\zeta]$ and $\Sigma[\zeta\zeta0]$ directions are shown in Fig. 4. The frequencies have been interpolated as described in Sec. 2.1, except for the 16 triple-axis results. The frequencies in units of 10^{12} sec^{-1} of some typical phonons are: TA(0,0,1.000), $\nu=4.39\pm0.04$; LO(0,0,0.984), $\nu=8.52\pm0.15$; TO(0.488, 0.488, 0.488), $\nu=6.19\pm0.07$, LA(0.988, 0.988, 0.0), $\nu=7.65\pm0.08$. The errors in the time-of-flight results were between 1 and 2%, and were computed from the standard deviations of the centers of gravity of the fitted Gaussians. They are therefore determined by the number and distribution of counts within the peak, and in the surrounding background. The observed sactter in time-of-flight results, on the other hand, was found to have a standard deviation approximately 1.6 times as large as the average computed error. This factor is presumably an indication of systematic errors and should be applied to the computed errors in making comparisons. The percentage errors increase markedly for modes of high frequency such as the LO branches, because the fractional error in measuring the shorter time-of-flight is greater, and also because the intensity of the neutron

[13] B. N. Brockhouse, in *Inelastic Scattering of Neutrons in Solids and Liquids* (International Atomic Energy Agency, Vienna, 1961), p. 113.

[14] D. H. Saunderson, C. Duffill, and R. I. Sharp, Atomic Energy Research Establishment Harwell Report No. AERE-R4895, 1965 (unpublished).

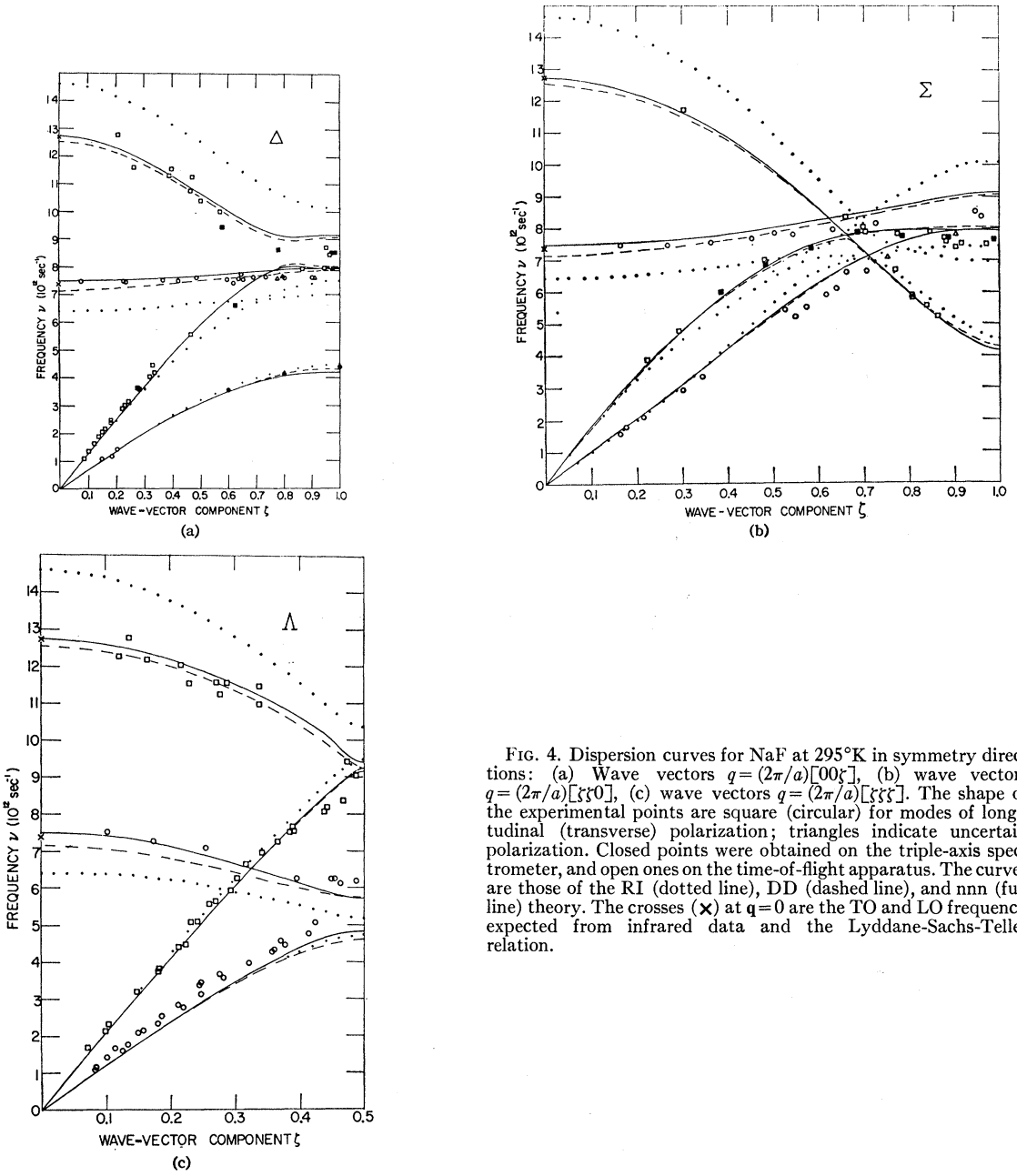

FIG. 4. Dispersion curves for NaF at 295°K in symmetry directions: (a) Wave vectors $q=(2\pi/a)[00\zeta]$, (b) wave vectors $q=(2\pi/a)[\zeta\zeta 0]$, (c) wave vectors $q=(2\pi/a)[\zeta\zeta\zeta]$. The shape of the experimental points are square (circular) for modes of longitudinal (transverse) polarization; triangles indicate uncertain polarization. Closed points were obtained on the triple-axis spectrometer, and open ones on the time-of-flight apparatus. The curves are those of the RI (dotted line), DD (dashed line), and nnn (full line) theory. The crosses (×) at $\mathbf{q}=0$ are the TO and LO frequency expected from infrared data and the Lyddane-Sachs-Teller relation.

groups is reduced. The errors quoted for the triple-axis results are estimated from the general appearance, principally the shape and breadth, of the observed neutron groups. Purely statistical arguments would indicate a smaller standard deviation, as was found in the time-of-flight spectra.

3.1 Comparison with Theory

The lattice dynamics of alkali halide crystals has been represented in two nearly equivalent formulations: the shell model used by Woods *et al.*[3] and the deformation-dipole model of Karo and Hardy.[6] Both models, within the framework of the harmonic and adiabatic[15] approximations, attempt to describe the effect of the readjustment of the outer electrons on the motion of the lattice wave. The models involve the Coulomb interactions of dipoles situated on the atoms the magnitude of the dipoles being determined by the electric field and the overlap forces. In this section we compare the results with models used by Karo and Hardy, deferring discussion of the shell model to Sec. 3.2.

[15] M. Born and K. Huang, in *Dynamical Theory of Crystal Lattices* (Oxford University Press, Oxford, England, 1954).

The meaning of the parameters used by Karo and Hardy, given in Table I, is as follows. In the deformation-dipole (DD) model with nearest neighbor interactions the deformation dipole is assumed to be produced entirely on the negative ion and proportional to the overlap potential $Ae^{-r/\rho}$ in magnitude. The electrical polarizabilities α_+ and α_- of the Na^+ and F^- ions are regarded as independent, in contrast with the polarizabilities predicted by the shell-model. The work of Tessman, Kahn, and Shockley[7] indicates that this assumption is unsatisfactory for sodium fluoride, where the observed polarizability is 13% higher than that predicted by least-squares fitting of an additivity rule to all the alkali halides. The effective charge on the ions is chosen so that the dielectric constants and infrared absorption frequency satisfy the Szigeti relation.[15]

A recent extension to the DD model[16] has included second-neighbor forces and a type of three-body force. The resulting next-nearest-neighbor (nnn) model, originally introduced to explain the phase transition in RbI, might be thought to be relevant to NaF in view of the phase transition found at 18.3 kbars by Pistorius and Admiraal.[17] It may be noted that a transition at this pressure was not observed by Bridgman.[18]

As well as the DD and nnn models, the results of a rigid ion (RI) theory[19] have also been compared with the experiment.

The three versions of the theory were calculated by Hardy and Karo.[20] The resultant frequencies for the DD model differ considerably from those quoted by the same authors[6] earlier; for example, the discrepancy of 24% between the frequency of the TO mode, calculated from the earlier theory, and the restrahl frequency has now been removed.

In Fig. 4 the three models discussed above are compared with experiment. We first examine the relation of the frequencies of the optical branches at long wavelengths to the results of independent experimental techniques. The LO and TO frequencies for long wavelengths expected from the infrared absorption frequency and the dielectric data quoted by Martin[21] are shown as crosses at $\mathbf{q}=0$ in Fig. 4. The low-frequency dielectric constant ($\epsilon_s=5.10$) used was that determined at audio-frequencies by Haussuhl,[22] rather than the value ($\epsilon_0=4.5$) obtained by fitting of the Lorentz dispersion formula to the main infrared absorption peak. The difference between the two values has not been satisfactorily explained. Table II shows that the neutron results extrapolated to $\mathbf{q}=0$ agree with the infrared absorption frequency to within 1.8%. They also satisfy the Lyddane-Sachs-Teller relation[23]

$$(\epsilon_\infty/\epsilon_\infty)^{1/2}=(\nu_{LO}/L_{TO})$$

to 2.3%, which is within the experimental error.

TABLE I. Input parameters used in the calculations of Hardy and Karo for sodium fluoride at room temperature.

Parameters	Value
Electrical polarizability[a]:	
Positive ion	$\alpha_+=0.255$ Å^3
Negative ion	$\alpha_-=0.759$ Å^3
Elastic constants[b]:	
	$C_{11}=9.71\times10^{11}$ dyn/cm^2
	$C_{12}=2.43\times10^{11}$ dyn/cm^2
	$C_{44}=2.80\times10^{11}$ dyn/cm^2
Dielectric constants:	
Low frequency[c]	$\epsilon_0=5.10$
High frequency[a]	$\epsilon_\infty=1.739$
Absorption frequency[d]	$\omega_0=4.64\times10^{13}$ rad/sec.
Derived parameters:	
Effective charge	$e^*/e=0.827$
Screening radius	$\rho=0.2888$ Å

[a] Reference 7.
[b] K. Spangenberg and S. Haussuhl, Z. Krist. **109**, 4 (1957).
[c] S. Haussuhl, Z. Naturforsch. **12a**, 445 (1957).
[d] Reference 15.

At all wave vectors it may be seen from Fig. 4 that the rigid-ion model gives very poor agreement with experiment for all three symmetry directions. The discrepancies are greatest for the LO mode which is consistently high (15% at [0,0,0] and 19% at [0,0,1]) and the TO mode which is consistently low (15% at [0,0,0] and 16% at [0.5,0.5,0.5]). Thus the rigid-ion model is just as unsatisfactory in sodium fluoride, where the polarizability is low, as it is in more polarizable crystals such as NaI, KBr,[3] and NaCl[4].

Comparison with the DD model shows a marked improvement in the agreement between theory and experiment. For regions of the dispersion curves away from zone boundaries, the model reproduces the longitudinal modes extremely well but is not so satisfactory for transverse modes. The longitudinal optical mode along [00ζ] is 5% high as the zone boundary is approached, although the acoustic mode is well reproduced. At [001], the DD splitting in the longitudinal modes is 1.8 times the splitting found experimentally.

The TO modes appear to be much flatter than is predicted by theory. The discrepancy is evident at the zone boundary in all three symmetry directions and is typically 6% in magnitude. Of the transverse acoustic

TABLE II. Comparison with infrared absorption frequency and the Lyddane-Sachs-Teller realtion.

ν_{LO} ($\mathbf{q}\to0$) Neutrons (10^{12} sec^{-1})	ν_{TO} ($\mathbf{q}\to0$) Neutrons (10^{12} sec^{-1})	ν_{TO} ($\mathbf{q}\to0$) Infra-red (10^{12} sec^{-1})	$(\epsilon_s/\epsilon_\infty)^{18-2}$	$(\nu_{LO}/\nu_{TO})_{\mathbf{q}\to0}$ Neutrons
12.65±0.35	7.51±0.08	7.38	1.72	1.68±0.07

[16] J. R. Hardy and A. M. Karo, in *Lattice Dynamics*, edited by R. F. Wallis (Pergamon Press Inc., New York, 1965), p. 195. A. M. Karo and J. R. Hardy, Phys. Rev. **141**, 696 (1966).
[17] W. F. T. Pistorius and L. J. Admiraal, Nature **201**, 1321 (1964).
[18] P. W. Bridgman, *The Physics of High Pressures* (G. Bell and Sons, London, 1952).
[19] A. M. Karo, J. Chem. Phys. **31**, 1489 (1959).
[20] J. R. Hardy and A. M. Karo, Phys. Rev. (to be published).
[21] D. H. Martin, Advan. Phys. **14**, 39 (1965).
[22] S. Haussuhl, Z. Naturforsch. **12a**, 445 (1957).
[23] R. H. Lyddane, R. G. Sachs, and E. Teller, Phys. Rev. **59**, 73 (1941).

TABLE III. Results of shell-model fitting. Parameters not followed by an error estimate were held fixed during the fitting procedure at the values indicated. The notation is that of the Appendix.

	Short-range forces (units $e^2/2v$)						Ionic charge	Polarizability				
	Nearest neighbors		Second-nearest neighbors					Electrical Na	Short range	Electrical F	Short range	Goodness of Fit
			Sodium-Sodium		Fluorine-Fluorine							
Model	A	B	A'	B'	A''	B''	(Units e) Z	(10^{-24} cm^3) α_+	Na (units e) d_+	(10^{-24} cm^3) α_-	F (units e) d_-	χ
I (a)	9.536	−1.165	0.00	0.00	0.00	0.00	1	0.00	0.00	1.21	0.2215	6.73
I	10.37 ±0.02	−1.065 ±0.008	0.00	0.00	0.00	0.00	1	0.00	0.00	1.21	0.2215	1.98
II	10.37 ±0.03	−1.075 ±0.010	0.00	0.00	0.00	0.00	1	0.00	0.00	1.15 ±0.03	0.206 ±0.007	1.99
VI	9.26 ±0.19	−0.77 ±0.05	0.00	0.00	0.34 ±0.08	−0.02 ±0.02	0.907 ±0.015	0.27 ±0.10	0.01 ±0.01	0.70 ±0.08	0.116 ±0.015	1.68

modes, the best agreement is obtained for the [001] direction, the theory being too low in the [111] direction and too high in the [110] direction.

The DD model is therefore seen to give a good description of the dispersion curves of NaF except near zone boundaries where the differences typically amount to 6%.

The calculations based on the nnn model can be seen from Fig. 4 to produce frequencies so close to those of the DD model that no significant improvement in agreement with experiment is achieved. The comparison between experiment and DD theory given in the previous paragraphs is therefore applicable to the nnn model also. The weakness of the second-neighbor interactions might have been expected from the relative ionic radii in sodium fluoride. No features have been seen in the results which would indicate that any mode might become unstable under pressure.

3.2. Shell-Model Claculations

The results in symmetry directions have been fitted by least-squares refinement of the parameters of several versions of the shell model. The equations of motion and definitions of the parameters, described in the Appendix are essentially those given by Cowley *et al.*[3] The parameters of the fitted shell-models that have been obtained are not simply related to the DD or nnn parameters, as the models are based on different equations of motion.[3] The most general shell model used includes first- and second-neighbor short-range forces between ions, short-range and electrical polarizability, and Coulomb forces between point dipoles.

The parameters of the more important models are summarized in Table III. They were adjusted to give the best fit to the observed frequencies interpolated to evenly spaced points on the symmetry directions. Five observations per branch of the dispersion relations were used as input data. A high-frequency dielectric constant[21] of 1.72±0.05 was also used. It should be noted that the models were not fitted to the ultrasonically determined elastic constants, unlike the fitting procedure used for KBr and NaI. The quantity χ is the ratio of the error in frequency of the model to the estimated experimental error. It is given by

$$\chi^2=\frac{1}{n(\text{Obs})-n(\text{Fit})}\sum^{n(\text{Obs})}\left(\frac{\nu^2(\text{Model})-\nu^2(\text{Observed})}{\sigma(\nu^2)}\right)^2$$

where n(Obs) is the number of observations, n(Fit) is the number of fitted parameters, and $\sigma(\nu^2)$ is the standard error in ν^2.

Model I(a) is the simple shell model[3] in which only the negative ion is allowed to deform and central nearest-neighbor interactions are considered; its parameters were not fitted but were determined from the lattice constant, elastic constant[24] C_{11}, and [21]high- and [22]low-frequency dielectric constants. The frequencies of the model differ significantly from the experimental ones, particularly for TO modes, as shown in Fig. 5.

However, the simple shell model predicts phonon frequencies in NaF that are much more accurate ($\chi=6.73$) than those predicted for NaI ($\chi=15.4$) and KBr ($\chi=55$). It is therefore clear that this simple version of the shell model is more satisfactory in materials whose polarizability is low, as was mentioned in the introduction.

Model I differs from I(a) in that the parameters of the nearest-neighbor short-range force (A and B) are allowed to vary; they change by about 10% in order to fit the acoustic branches at long wavelengths. The results of model II in which the electrical (α_-) and distortion (d_-) polarizability of the negative ion are also varied, confirm these values for A and B, and for α_- and d_-, which remain within 5% of their previous values.

Model II is still the simple shell model, but it differs from I(a) in having been fitted to the experimental frequencies and dielectric constant. The error of the model ($\chi=1.99$) is very low compared with model I(*a*) because the fitting has produced better agreement with the elastic constant region of the dispersion curves. This conclusion is borne out by Table IV, which contains

TABLE IV. Elastic and dielectric constants of sodium fluoride.

Source	C_{11}[c]	C_{12}	C_{44}	ϵ_∞
Model I(a)	8.96	2.82	2.82	1.78
Model I	10.64	2.62	3.02	1.78
Model II	10.65	2.63	3.00	1.73
Model VI	10.89	2.40	2.98	1.60
Ultrasonic[a] and optical[b]	9.70	2.43	2.80	1.72

[a] S. Haussuhl, Z. Physik **159**, 223 (1960).
[b] D. H. Martin, Advan. Phys. **14**, 39 (1965).
[c] Elastic constants are in units of 10^{11} dyn cm^{-2}.

[24] S. Haussuhl, Z. Physik **159**, 223 (1960).

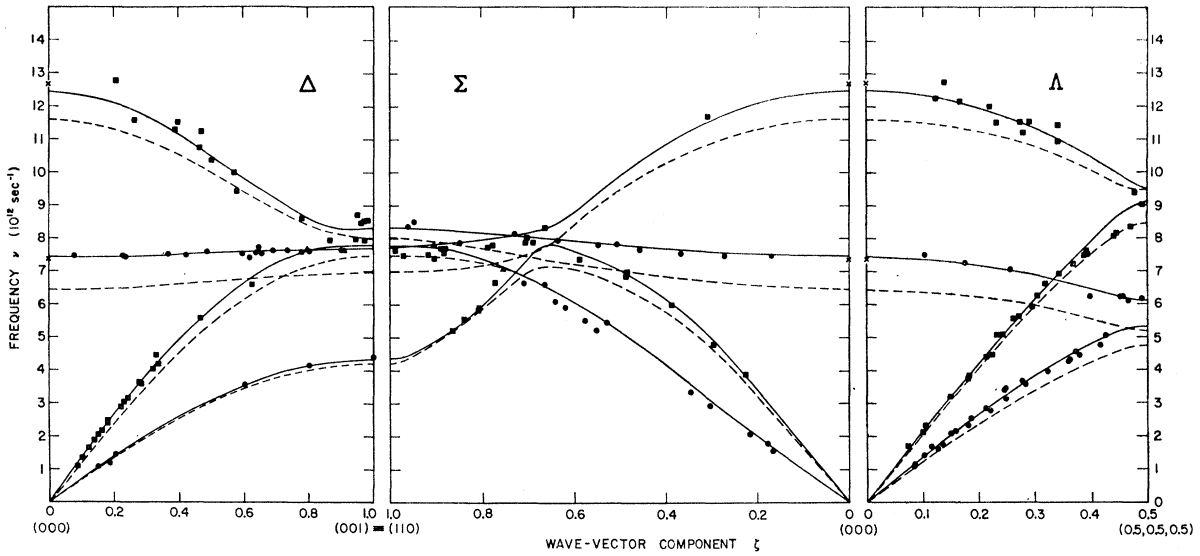

FIG. 5. Results of shell-model fitting. The solid line refers to model VI, and the broken line to the simple shell model.

the elastic constants predicted by some of the models, as well as those obtained from ultrasonic measurements. The value of C_{11} of model II is in agreement with the values of all the models fitted to frequencies deduced from thermal neutron scattering; it is 9.8% higher than the ultrasonic value of C_{11}.

Models III to VII allow for positive ion electrical and short-range polarizability, second-neighbor short-range interactions between ions, and an ionic charge different from unity. As these models all gave quite similar χ values, only results for the best one are given. Model VI was selected as the best fit to the results and is shown as the full line in Fig. 5. It has a small second-neighbor interaction between fluorine ions; the ionic charge of $0.91e$ is determined by the least-squares fitting to $2\frac{1}{2}\%$. The ratio A''/A is characteristic of exponentially varying exchange interaction rather than Van der Waals interaction.

Finally it should be mentioned that the parameters obtained by fitting to experimental results are physically significant only to the extent that the shell model is valid for sodium fluoride. A given model, however, is useful as a means of interpolation of results to the accuracy specified in the goodness of fit. Thus the frequencies at a selection of wave-vectors off symmetry directions have been calculated from Model VI, and are compared with the observed phonon frequencies obtained from the time-of-flight data in Table V. From a total of 37 such phonon frequencies, the value 2.84 for the average error, χ (off-sym), that the model VI makes in predicting the observed frequencies has been obtained. Thus the fit in off-symmetry directions is not so good as the fit ($\chi=1.68$) in symmetry directions. This reflects the larger systematic (i.e., not included in the computed σ) error in an individual observed frequency than in the averaged frequencies used for the fitting procedure in symmetry directions. The fit in off-symmetry directions is sufficiently close to show that model VI does provide a satisfactory means of obtaining any frequency within the Brillouin zone.

TABLE V. Phonon frequencies in off-symmetry directions calculated from model VI, compared with observed frequencies obtained from time-of-flight spectra. Under the heading "mode type," the figure gives the number of the branch in order of increasing frequency for the four branches observable in the (1̄10) scattering plane; the letters give the polarization of the mode only approximately, for the exact polarization in off-symmetry directions is neither longitudinal nor transverse.

Wave vector $\mathbf{q}=(2\pi/a)(\xi,\zeta,\eta)$		Frequencies (Units 10^{12} cps)		Mode type	Deviation
ζ	η	ν (Obs)	ν (Model)		$[\nu$ (model)$-\nu$ (Obs)$]/\sigma$
0.0849	0.5081	6.02±0.04	6.02	2, LA	−0.14
0.1350	0.9881	5.20±0.04	5.15	1, TA	−1.25
0.1718	0.5564	4.53±0.03	4.41	1, TA	−4.59
0.2050	0.3902	3.80±0.03	3.77	1, TA	−0.96
0.3847	0.6676	9.14±0.10	9.28	4, LO	+1.53
0.2670	0.3222	3.87±0.02	3.74	1, TA	−5.57
0.4393	0.5295	5.29±0.07	5.34	1, TA	+0.69
0.3058	0.2631	3.72±0.03	3.68	1, TA	−1.48
0.5042	0.4384	5.16±0.09	5.28	1, TA	+1.25
0.2715	0.2118	5.41±0.08	5.22	2, LA	−2.32
0.5220	0.3531	8.09±0.10	8.68	3, LA	+5.82
0.6081	0.2594	8.98±0.12	9.03	4, LO	+0.42
0.4064	0.0600	6.55±0.06	6.26	2, LA	−5.21

4. CONCLUSION

Measurements of inelastic neutron scattering from sodium fluoride at room temperature have been made using time-of-flight apparatus and a crystal spectrometer. The frequencies obtained are consistent, and demonstrate the inadequacy of the rigid-ion model even in a crystal of low polarizability. A relatively simple model of the forces, the DD model of Hardy and Karo,

in which short-range deformation polarizability is considered, is in good agreement with experiment. The discrepancies that remain do not exceed 6% and are most noticeable for transverse modes. Introduction of next-nearest-neighbor interaction does not significantly improve the agreement. The results are well fitted by a shell model containing nine parameters, in which the ionic charge is significantly less than unity.

ACKNOWLEDGMENTS

I am indebted to AERE (Harwell) where most of this work was carried out, and to Dr. P. A. Egelstaff who made extensive facilities available to me. I should also like to thank D. H. Saunderson, D. Long Price, and R. Sharp for much assistance and useful discussion. J. R. Hardy and A. M. Karo kindly supplied versions of their theory using an improved set of input parameters. Advice on the shell-model fitting was given by R. A. Cowley. The large crystal of sodium fluoride was grown by D. A. Jones of Aberdeen University.

APPENDIX

The shell-model equations of motion in matrix form of Cowley *et al.*[3] are

$$\mathbf{m}\omega^2\mathbf{U}=(\mathbf{R}+\mathbf{ZCZ})\mathbf{U}+(\mathbf{T}+\mathbf{ZCY})\mathbf{W}, \tag{A1}$$

$$0=(\mathbf{T}^T+\mathbf{YCZ})\mathbf{U}+(\mathbf{S}+\mathbf{YCY})\mathbf{W} \tag{A2}$$

where **U** is the amplitude of displacement of the ions and **YW** is the electronic dipole moment on the ions. **C** is the matrix of Coulomb coefficients while **R**, **S**, and **T** (together with its transpose $\mathbf{T}^T$) specify the short-range interactions. **m**, **Z**, and **Y** are diagonal matrices specifying the mass, ionic charge, and the charge on the shells.

Although Eqs. (A1) and (A2) are the general equations of the dipole approximation, they may also be obtained by considering rigid shells of charge Y to be isotropically bound with spring constant k to the ion cores, and to be interacting with other cores through the matrix **T**. One can then define electric polarizabilities α by

$$\alpha_+=\frac{Y_1^2}{k_1+(T_{11})_{q=0}}, \quad \alpha_-=\frac{Y_2^2}{k_2+(T_{22})_{q=0}} \tag{A3}$$

and short-range polarizabilities by

$$d_+=-\frac{(T_{11})_{q=0}Y_1}{k_1+(T_{11})_{q=0}}, \quad d_-=-\frac{(T_{22})_{q=0}Y_2}{k_2+(T_{22})_{q=0}}. \tag{A4}$$

The short-range interactions between nearest neighbors are specified by longitudinal and transverse restoring force constants A and B, which may be written

$$\left(\frac{\partial^2 V_{12}}{\partial r^2}\right)_{\parallel}=\frac{e^2A}{2v}, \quad \left(\frac{\partial^2 V_{12}}{\partial r^2}\right)_{\perp}=\frac{e^2B}{2v}. \tag{A5}$$

In the least-squares fitting analysis A and B are allowed to vary independently. The second-neighbor forces are given by four parameters. For the positive ions we have

$$\left(\frac{\partial^2 V_{11}}{\partial r^2}\right)_{\parallel}=\frac{e^2}{2v}A' \quad \left(\frac{\partial^2 V_{11}}{\partial r^2}\right)_{\perp}=\frac{e^2}{2v}B' \tag{A6}$$

and for the negative ions

$$\left(\frac{\partial^2 V_{22}}{\partial r^2}\right)_{\parallel}=\frac{e^2}{2v}A'' \quad \left(\frac{\partial^2 V_{22}}{\partial r^2}\right)_{\perp}=\frac{e^2}{2v}B''. \tag{A7}$$

The model now contains eleven parameters: six short-range parameters A, B, A', B', A'', B'', two crystal polarizabilities α_+, α_-, two short-range polarizabilities d_+, d_-, and the ionic charge Z.

The short-range interaction was assumed to act through the outer electrons by making the **R**, **S** and **T** matrices identical for all wave vectors.